Observation of Dugdale cracks in glass foils – a method for studying surface plasticity of soda-lime glass

The physical and chemical properties of subsurface layers on solids usually differ from bulk properties; they can considerably influence the qualities of materials such as strength and corrosion resistance. Especially in case of alkaline silicate glass there is a subsurface layer formed by contact with humid air [1–3] which behaves in a relatively ductile manner as demonstrated by scratching the surface [4]. Bishop [5] was the first to show the existence of a 500 Å thick low refractive layer on the surfaces of alkaline silicate glass specimens. Characterization of the composition and structure of a glass surface was made possible by development of new surface analysis methods, for example Auger electron spectroscopy, low angle infra-red reflection spectroscopy, X-ray microanalysis, etc. [6]. According to detailed studies of Hench [6] there are different types of surfaces. In all of them a more or less thick silica rich film is formed within a few minutes by surface hydration and selective alkali ion removal. Thickness and stability of these films are essentially dependent on glass composition, temperature, environmental humidity and reaction time. Glasses used in our work are supposed to have a chemically changed 500 to 900 Å thick surface layer resulting from contact with ordinary atmosphere, i.e. humid air [7].

To study the elastic–plastic behaviour of such sub-surface layers we prepared thin soda-lime glass foils of a thickness of about 1000 Å. Thus the two sub-surface layers forming by contact with humid air from both sides will penetrate the whole foil volume. In HVEM (high voltage electron microscope JEM 1000) the regions around the tip of artificially introduced cracks were studied. Elastic–plastic behaviour should then give rise to the formation of plastic zones. On the basis of the Dugdale model, if measured values of plastic zone size or COD, respectively, are used, the yield stress of the material can be determined.

Small plates of commercial container glass of 0.2 mm initial thickness were chemically thinned down to 10 μm by 40% fluoric acid at room temperature. Then chemical thinning was followed by ion beam milling in an IBM A 2 apparatus (AR^+ ions, 6 kV, 50 μA). As shown in Fig. 1 thinning

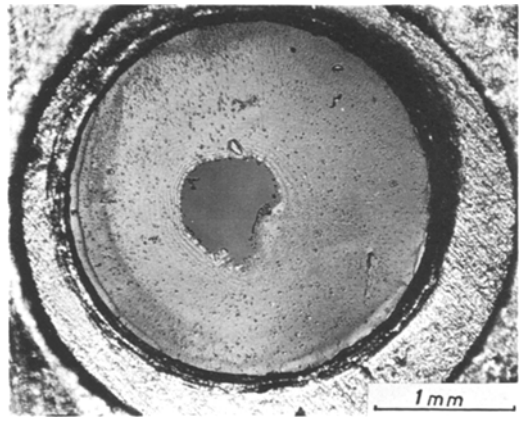

Figure 1 Ion beam thinned glass specimen.

was continued until a small hole in the middle of the specimen appeared. From visible interference fringes the thinned area can be deduced to be wedge shaped. At the border of the hole the wedge is blunted. There the initial material thickness is approximately 300 Å, and the wedge angle is 0.2°. The thickness increases nearly uniformly in a radial direction. Up to a distance of 20 μm from the border of the hole the material thickness is smaller than 1000 Å. Crack tip areas in foils prepared in this way were examined in a HVEM at 1000 kV. Previous investigations have shown that glass foils of the above-mentioned thickness cannot be studied in a 100 kV electron microscope. The main disadvantage is the required high beam current (up to 70 μA) causing a strong local specimen heating up to temperatures of 700° C, leading to structural changes of the glass. Contrary to this the specimen temperature in the HVEM at 1000 kV (5 μA beam current) is less than 100° C [8], i.e. mechanical and structural properties are not influenced.

Typical features were observed around crack tips in foil areas of a thickness smaller than 1000 Å (Fig. 2). The crack tip is strongly blunted, and in front of the crack a narrow region marked by contrast brightening can be observed. The crack tip blunting indicates plastic deformation according to Dugdale's observation [9] of metal plates under plane stress conditions. Brightening of the region in front of the crack tip should characterize the plastic zone according to the Dugdale model: Plastic flow causes a necking of the foil material within these zones, i.e. the decrease in foil thickness leads to a more or less brightening because of the decreased absorption of the imaging

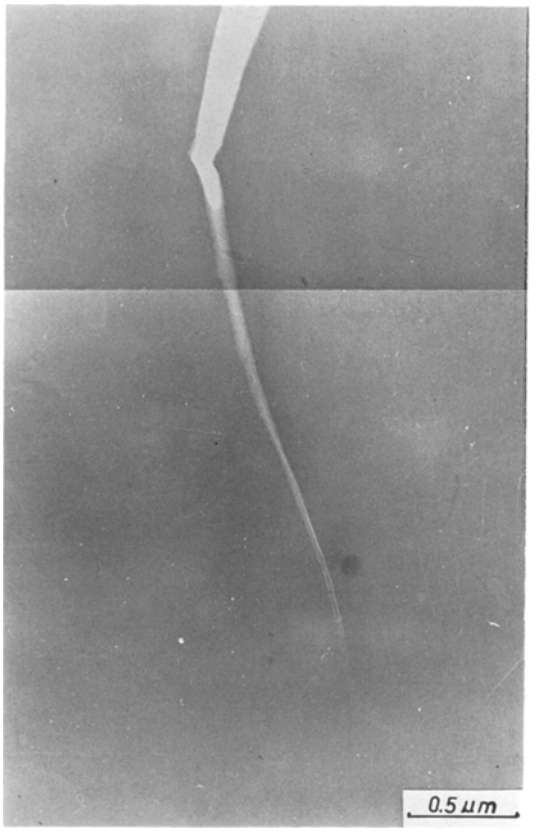

Figure 2 Crack with plastic zone in a glass foil.

electrons. Similar electron microscopic observations of foil necking within plastic zones were made in metal and polymer foils [10–12].

The orientation of the crack plane could be determined by tilting the glass specimens in the HVEM stage. Only cracks having a crack plane orthogonal to the foil plane were used for interpretation. Also, it could be proved that the observed crack contours were not due to contamination. Within the observation time (up to 20 min at the most) contamination did not occur in the HVEM at a magnification of 10 000 × and a beam current of 5 µA.

The yield stress σ_y of the foil material can be calculated after Dugdale [13] as

$$\sigma_y = \frac{\pi E V(c)}{4c \ln (a/c)} \quad (1)$$

using the open crack length c, the length of the crack plus plastic zone length a, the crack tip opening $2V(c)$ and Young's modulus E. The crack data, according to Fig. 2, are: $c = 8.1\,\mu m$, $a = 11.1\,\mu m$ and $V(c) = 0.05\,\mu m$. Taking for E the Young's modulus of the bulk glass ($E = 68\,375\,N\,mm^{-2}$) one obtains the yield stress $\sigma_y = 1051.6\,N\,mm^{-2}$ from Equation 1. The finite and special specimen geometry of the glass foils used in our experiments might lead to the relationship between σ_y and the other quantities deviating from that in Equation 1. The foil radius r is 1.5 mm. The crack illustrated in Fig. 2 runs in an outer radial direction from the border of the hole having a radius $R = 26.5\,\mu m$. Thus

$$R/r = 0.019; \quad c/r = 0.0054; \quad R/c = 3.5. \quad (2)$$

Kuna [14] has studied the influence of a finite specimen geometry, similar to our foil geometry, on Dugdale's Relation 1. The calculations were made using a finite element method applied to a square disk with a central hole and two symmetric cracks (see Fig. 3). Of particular interest was the calculated case:

$$R/d = 0.071\ (\hat{=} R/r); \quad c/d = 0.035\ (\hat{=} c/r); \quad R/c = 2.4 \quad (3)$$

In Kuna's case the geometry should cause a much stronger deviation from Equation 1 than in the experimental case considered, whereas the influence of the central hole should be nearly the same in both cases. To study the geometrically caused deviations the normalized dimensionless crack tip opening $\delta = \pi E V(c)/4\sigma_y d$ is used, δ^* is the dimensionless opening according to Kuna's values and δ^{**} that according to Equation 1 (see Fig. 3). The relative error $f = \delta^* - \delta^{**}/\delta^{**}$ is drawn in the upper curve of Fig. 3. It can be seen that f approaches zero for $c/a \geqslant 0.83$, while for $c/a = 0.73$, f is about 70%. Strain and displacement fields in the crack tip vicinity are independent of the outer specimen geometry if one considers distances relatively small in comparison with the specimen dimensions. Therefore, to estimate the yield stress σ_y on the basis of Equation 1 we used values $c/a \geqslant 0.73$. According to the remarks on Relations 2 and 3 given above the deviations from the infinite case (Equation 1) should be smaller for the foils used here than in the case calculated by Kuna.

The computed σ_y values lie between 1020.2 N mm^{-2} and 2403.4 $N\,mm^{-2}$ for c/a values between

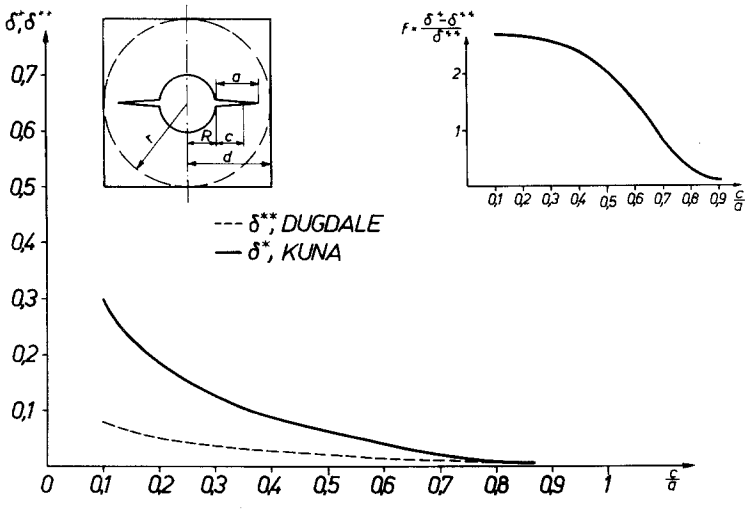

Figure 3 Plot of normalized crack opening δ versus ratio of open crack length to crack length with plastic zone, c/a.

0.73 and 0.87. Because of the large scatter a mean value was not determined. Several factors responsible for such large changes are to be considered: (i) The properties of glass surface layers are dependent on reaction time and environmental humidity (temperature and glass composition are constant) as mentioned above. Reaction time and humidity were different for different foils*. (ii) Changes of wedge angle and foil thickness could influence the yield stress determination. This, however, could be controlled on a large scale so that factors of point (i) are probably of greater importance. Besides, the true value of the Young's modulus of the subsurface layer is unknown. For estimation the Young's modulus of the surface layer is about 75% of the modulus of bulk quartz which will be about $55\,917\,N\,mm^{-2}$ [15]. Thus the yield stress σ_y might even be smaller than the values determined above.

In 1964 Marsh [16] estimated a yield stress of $\sigma_y = 4905\,N\,mm^{-2}$ for bulk glass of similar composition. It should be mentioned that the problem of plastic flow of bulk glass is not yet solved (see for example Ernsberger [17]). Marsh used DPH† values for determining the yield stress, while Grau *et al.* [18, 19] carried out microhardness experiments for determining DPH values of upper glass layers, and reported that the DPH values of these layers were up to 30 to 40% lower than those of bulk glass measured in the same way. Comparing the surface yield stress determined in this work with that of Marsh one finds a relative change of the subsurface versus bulk property comparable to that noticed by Grau (see also our previous report [20]).

Acknowledgement

The authors are indebted to Professor H. Bethge for supporting this work.

References

1. L. AINSWORTH, *J. Soc. Glass Techn.* 38 (1954) 479.
2. D. M. SANDERS and L. L. HENCH, *J. Amer. Ceram. Soc.* 56 (1973) 373.
3. L. L. HENCH, *J. Non-Cryst. Solids* 19 (1975) 27.
4. P. JOOS, *Z. Angew. Phys.* 9 (1957) 556.
5. F. L. BISHOP, *J. Amer. Ceram. Soc.* 27 (1944) 145.
6. L. L. HENCH, Xth International Congress on Glass, Prague 1977, Part I (ČVTS-Dum Techniky, Prague, 1977) p. 343.
7. C. G. PANTANO, Jr., D. B. DOVE and G. Y. ONODA Jr., *J. Non-Cryst. Solids* 19 (1975) 41.
8. J. HOPFE, diploma work, Halle (1974).
9. D. S. DUGDALE, *J. Mech. Phys. Solids* 8 (1960) 100.
10. V. SCHMIDT, A. SCHAPER, A. M. LEKSOWSKI and V. BETECHTIN, VIII. Arbeitstagung Elektronenmikroskopie, Berlin 1975 (Phys. Ges. der DDR, Berlin, 1975) p.303.
11. A. M. LEKSOWSKI, S. N. SAKIEV and V. SCHMIDT. *Fiz. Met. Metall.* 41 (1976) 637.
12. G. MICHLER and K. GRUBER, *Plaste Kautsch.* 23 (1976) 496.

*After ion beam milling the foils were exposed to laboratory air for a period between 2 h and 2 days before observation in the HVEM.

†DPH stands for diamond pyramid hardness.

13. A. S. TETELMAN and A. J. McEVILY, Jr., "Fracture of Structural Materials", (John Wiley & Sons, New York, 1967) p.62.
14. M. KUNA, thesis, Halle (1977).
15. L. L. HENCH, Private communication (1977).
16. D. M. MARSH, *Proc. R. Soc. London A* **279** (1964) 420.
17. F. M. ERNSBERGER, Xth International Congress on Glass, Prague 1977, Part I (ČVTS-Dum Techniky, Prague, 1977) p.293.
18. P. GRAU, Tagung "Strukturabhängiges Verhalten von Festkörpern", Dresden 1976 (Akademie Verlag, Berlin) to be published.
19. F. FRÖHLICH, P. GRAU and W. GRELLMANN, *Phys. Stat. Sol. (a)* **42** (1977) 79.
20. V. SCHMIDT, J. HOPFE and G. KÄSTNER, VIII. Arbeitstagung Elektronenmikroskopie, Berlin, 1975 (Phys. Ges. der DDR, Berlin, 1975) p.361.

Received 28 October
and accepted 14 November 1977.

V. SCHMIDT
J. HOPFE
Institut für Festkörperphysik und Elektronenmikroskopie der AdW der DDR, Weinberg 2, Halle/Saale, DDR

Thermal decomposition of $CaCO_3$ and formation of β-Ca_2SiO_4

β-Ca_2SiO_4 is an important cementing mineral of ordinary Portland cement (OPC) and has the potential to improve the quality of OPC by suitable modification of its structure, leading to partial or complete replacement of the most important high temperature cementing material, Ca_3SiO_5, in OPC. Examples are available where OPC of Indian and other origins show high early strength properties in spite of its low Ca_3SiO_5 content, mainly due to the presence of reactive β-Ca_2SiO_4, which was formed rather accidentally and thus could not be produced under controlled conditions.

Synthesis of β-Ca_2SiO_4 of reactive nature have recently been reported [1, 2]. In this communication it is intended to report the preliminary results on the decomposition of $CaCO_3$ and on the formation of β-Ca_2SiO_4 in the presence of NaF under different thermal treatments. The main objectives are:

(1) to improve the kinetics of the reaction between SiO_2 and CaO and increase the yield of the reaction product at a lower temperature with a low retention time

(2) to synthesize reactive β-Ca_2SiO_4 using normal raw materials

In doing so, the important steps taken consisted of (i) decomposing $CaCO_3$ at a lower temperature in the presence of SiO_2 + NaF and (ii) firing the products thus obtained to different temperatures adopting different heating schedules as suggested in [3, 4].

Reagent grade $CaCO_3$ and NaF were used with silica gel of fairly high purity for the synthesis of β-Ca_2SiO_4. The ratio of $CaCO_3$:SiO_2 was maintained approximately at 2:1. The materials were ground to powder (–325 mesh) before and after firing. Pelleting to a pressure of about 700 kg cm^{-2} was done for some of the mixes. The mixes were fired in a Pt-crucible in an electric furnace. The analysis of the materials was performed using differential thermal analysis (DTA apparatus, MoM, Hungary), X-ray diffraction (XRD apparatus, Phillips, Holland), and infra-red spectroscopy (i.r. apparatus, Perkin Elmer 621).

The effect of the addition of NaF on the decomposition of $CaCO_3$ can be seen in Figs. 1 and 2. The decrease in the decomposition temperature of $CaCO_3$ with increasing amount of NaF is considerable, although there is a sudden change in the mechanism of formation of compounds as is evident from Fig 2. The change in the slope of the curve at 10% NaF indicates the change in the compound formation or solid solution, the exact nature of which is yet to be established. The mix samples containing 6% or 12% NaF heated to 530 or 510° C (below the decomposition of $CaCO_3$, an endothermic DTA peak has been observed at this temperature, the intensity of which increases with increasing NaF content in the mix) showed quite interesting XRD patterns compared to that obtained at room temperature (Fig. 3). The XRD lines (2θ) at 26.1°, 27.1°, 45.9°, 50.1°, 52.4° and 52.9° of the mix at room temperature disappear completely from those of the heated samples. These lines are due to the presence of aragonite. The NaF line